Journal of Advanced Joining Processes 7 (2023) 100139

Contents lists available at ScienceDirect

Journal of Advanced Joining Processes

journal homepage: www.sciencedirect.com/journal/journal-of-advanced-joining-processes

A review: Suppression of the solidification cracks in the laser welding process by controlling the grain structure and chemical compositions

Mohammadhossein Norouzian *, Mahdi Amne Elahi, Peter Plapper

University of Luxembourg, 6, rue Coudenhove Kalergi, L-1359, Luxembourg

ARTICLE INFO

Keywords:
Solidification crack
Laser welding
Grain structure
Chemical compounds
Brittle intermetallic compounds
Suppression of cracks

ABSTRACT

Laser beam welding of miscellaneous material combinations is an effective joining technology useful for diverse industrial applications because it can provide high speed, flexibility, and precision. However, welding defects like solidification cracking are some of the challenges in the joining process. The past decade has seen an extended effort to deal with this issue in many studies. However, there remains to be more comprehensive research regarding preventive procedures for solidification cracking by changing the grain structure. Following a thorough understanding of the solidification crack mechanism theories, we reviewed recent research on the critical role of metallurgical factors in the solidification cracks during laser welding. It considers the influence of the grain structure, intermetallic compounds, and laser welding parameters to propose preventive procedures to suppress the solidification cracks. Recent achievements show grain refiners, laser beam oscillation, ultrasonic vibration, and implementation of double laser sources are the main strategies that suppress or minimize solidification cracks. Furthermore, in laser beam welding of dissimilar materials, like steel-hard metal and copper-aluminum, brittle intermetallic compounds are recognized as one of the main reasons for the solidification crack susceptible increment. Recent approaches to overcome the formation or reduce the number of intermetallic compounds through various laser parameters and setups are discussed.

Introduction

Laser Beam Welding (LBW) is a rapid, precise, and non-contact method to join components. This technology makes the welding of conductive, dissimilar, and reflective materials feasible (Katayama, 2020). Heat Affected Zone (HAZ) and material distortion are lessened because of the outstanding control over energy input in the fusion zone (Katayama, 2013). The ability to achieve high-quality and narrow welds at high production rates makes the laser beam a promising welding technology (Cicală et al., 2005). Laser welding applications have been reported for miscellaneous material combinations in many investigations. For instance, Laser welding of metals to polymers is studied, and the effect of laser-based surface treatments on promoting the physiochemical bonding at the interface and the parameters affecting the mechanical performance of the joints are investigated (Amne Elahi et al., 2021). Laser welding of hard metals to steel for cutting tools on butt joints is achieved by considering the effect of the vertical focal point position, welding power, and velocity (Costa et al., 2003). Laser welding of dissimilar metals for micro welding applications and the impact of different laser beam trajectories on joint quality and mechanical properties is also reported (Amne Elahi and Plapper, 2019). Recent development in laser welding promises a joining process for aluminum-steel. Although the mechanical performance of this dissimilar joint is limited, the laser sources provide high flexibility and accurate control of heat input (Wallerstein et al., 2021).

With increasing the efficiency of the laser sources and quality of laser beams, laser welding applications are being used in several industrial areas. However, welding defects or imperfections that cause a fracture in welded parts may occur under undesired conditions. Depending on the materials used and their compositions, the welding process, fixture constraints, etc., many defects may arise in laser welding (Katayama, 2013).

Hot crack is one of the most well-known defects in the welding process. This term is prone to arbitrary and vague interpretation. In numerous studies, any crack occurring at a high temperature is frequently referred to as a "hot crack"; however, this is inaccurate. Three distinct types of cracking are specifically mentioned here when the phrase "hot cracking" is used: 1) Solidification crack: appears on the

* Corresponding author.
E-mail address: Hossein.norouzian@uni.lu (M. Norouzian).

https://doi.org/10.1016/j.jajp.2023.100139

Available online 18 January 2023

fusion zone at the end of the solidification phase. 2) Liquation crack: occurs in HAZ along the grain boundaries 3) Weld metal liquation crack: observed in multi-pass welding that results from grain boundaries remelting (Lippold, 2015).

Solidification cracks take place at the last stage of solidification. A complex interaction of mechanical, thermal, and metallurgical factors leads to the formation of this kind of crack (Wang et al., 2015). Due to the contribution of a stress concentration, solidification crack will lead to premature failure and fatigue. Thus, it is widely researched and has been the subject of numerous studies (Shankar and Devletian, 2005). Fig. 1 shows the melting and solidification processes that occur during laser welding on the workpiece and also depicts the "Mushy zone" (MZ), a two-phase region between solid and liquid areas (Wang et al., 2004). A residual liquid film emerges in the mushy zone, where there is a high misorientation angle among the grains. In thin liquid films, solidification cracks arise due to the thermal stresses and strains produced by solidification shrinkage and thermal contraction (Jonathan Dantzig, 2007; Han et al., 2021).

To fully comprehend, one must introduce three separated regions in the mushy zone specified in Fig. 1: 1) free liquid feeding, in which the liquid is easy to move. 2) restricted liquid feeding. This zone is vulnerable because liquid feeding is challenging, and the material's relatively low transverse shear strength. Hence, the liquid flow may not accommodate the thermal contraction of the solid and will result in the separation of dendrites. 3) coherent solid zone where the liquid feeding is stopped, and the liquid is present as solitary droplets between solid networks. The grain coalescence follows the attraction and repulsive forces when there is a thin residual liquid film among the grain boundaries (The term ''Attraction and repulsive'' refers to the grains joining when there is no need for energy to attract crystals or when the liquid film between the crystals must disappear). If the energy of the grain boundary is less than double of solid-liquid interface energy, the liquid film is unsteady, and dendrites integrate once reaching an interplay distance. Otherwise, the liquid film remains stable and separates the dendrites (Wang et al., 2004). At T_b^a(coalescence temperature), the attraction of intragranular coalescence boundaries occurs while, T_b^r is the temperature at which the liquid film remains stable. These temperatures are influenced by the solidification circumstances and material properties. Formula. 1 expresses the critical coalescence cooling temperature (Wang et al., 2004):

$$\Delta T_b = \frac{\gamma g_b}{\Delta S_f \delta} \tag{1}$$

Where γ_{gb} is the grain boundary energy, γ_{sl} is the solid-liquid interfacial energy, δ is the diffuse interface thickness, ΔS_f is the entropy of fusion per unit volume, and ΔT_b is the critical temperature that liquid film remains stable. Once this temperature difference crosses the critical temperature and the liquid film remains along solidification grain boundaries, a solidification crack appears (Wang et al., 2004).

Weld solidification cracking may be avoided or mitigated if the mechanism of solidification cracks, metallurgical aspects, and effective parameters of laser welding is well considered. All the mentioned solidification theories are based on the liquid film along grain boundaries in the last solidification phase. This review studies the mechanism of solidification cracks based on various theories. Then discusses the matter of grain structure, chemical composition and intermetallic compounds in the creation of the solidification cracking. Laser process parameters will be analyzed, and some practical preventive solutions will be proposed.

Solidification crack mechanism theories

Many theories focused on weld defect's mechanical or metallurgical aspect. The first theory is called "shrinkage-brittleness." It states that during the solidification process and in a high-temperature range, the liquid to solid ratio is high and the liquid phase surrounds dendrites. However, by the temperature dropping, to the coherence temperature (a temperature between solidus and liquidus), the solid initiate to interact and make a solid network. A high strain rate in the structure will develop at a temperature below coherence temperature due to solid-solid bridging and lack of feeding liquid. This temperature range between the solidus and coherence temperature is called the "effective interval." Based on this theory, Brittle Temperature Range (BTR) is located in the effective interval area. A solidification crack occurs when shrinking strains increase over a critical point in the BTR (Pumphrey, 1948).

"Strain theory" considered solid-liquid separation rather than solid-solid separation. According to this theory, solidification occurs in the mushy zone and the liquid film stage. In the mushy zone stage, the temperature is higher than that of the liquid film stage; therefore, it has a more significant liquid fraction. Under equilibrium solidification conditions, the residual liquid film becomes thinner in the liquid film stage compared to the early stage. Due to shrinkage and thermal contraction, the thin liquid layer cannot overcome the formed tensile strain at the grain boundaries leading to solidification cracking (Apblett WR, 1954).

Another theory by Borland (1960) also modified the shrinkage-brittleness theory called the "generalized theory." It states that the solidification process has four stages: 1) the mushy zone stage, where there is enough feeding of liquid and the primary dendrites appear 2) the coherence range, where the dendrites interlocked, and only the liquid phase can move and fill the boundaries. If cracks occur in this stage due to strain, there is still a chance to heal them with the thick liquid film. 3) critical solidification range that the solid is coalesced and builds a solid network. There is also less liquid phase 4) completed

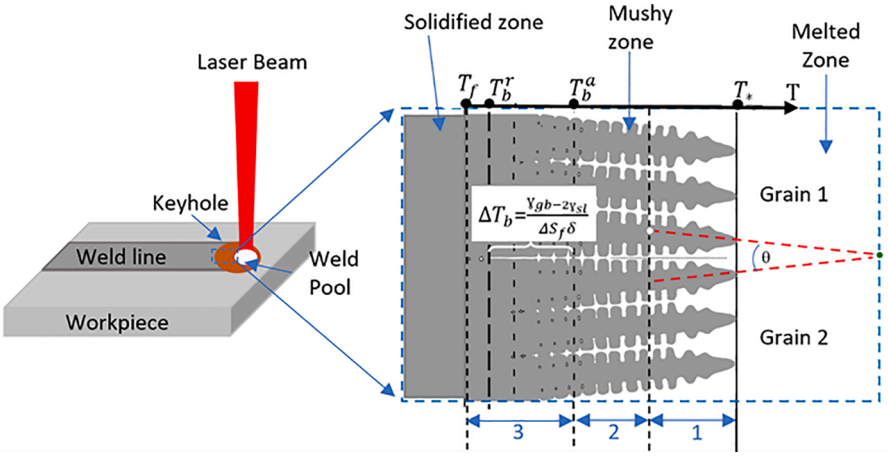

Fig. 1. Laser beam welding on the workpiece (left), solidified, mushy and melted zones (right) (Wang et al., 2004).

solidification, which is the last stage of solidification, and the solidification crack will appear if there is residual liquid film.

Generalize theory states that the presence of enough liquid might compensate for the failure of the solid-solid bridges, and "crack healing" is conceivable above the "critical" range. However, recovering is impossible below the coherent temperature due to insufficient liquid phase and an interlocked solid network inside the "critical" range. Therefore, solidification cracking is unavoidable. The theorist could also estimate and quantify the distribution of the liquid phase by considering the interfacial energy ratio or liquid wettability. Solid-liquid interface energy, solid-solid interface energy, and dihedral wetting angle are influential factors that clarify this interfacial energy ratio. Using this method, he could explain why the mushy stage is low in cracking susceptibility and the critical stage is highly susceptible (Manitsas and Andersson, 2018).

In 1982, the "modified generalized" theory was presented by Matsuda et al. (1982). In this theory, the first stage is narrower than what is proposed by the generalized theory. It means solid networks appear very rapidly below liquidus temperature. Fig. 2 illustrates four main stages of the solidification process. In stage 1, the solid is entirely surrounded by the thick liquid film. In stage 2, the liquid films have low dihedral angles on grain boundaries and the critical solidification is at this stage's highest temperature and boundary. Stage 3 is divided into the film stage (3H) and the droplet stage (3 L), where there are scattered residual liquids. The crack initiation is proposed in the 3H and the propagation of the crack is in the 3 L. In addition, Matsuda observed solidification cracks by metallography and proposed different types of fractures based on the material structure (Lippold, 2015).

The last proposed theory is the "technological strength theory" (Prokhorov and Prokhorov, 1971). This theory is particularly helpful in describing the ductility/strain contribution to solidification cracking, even if it does not address the metallurgical or fracture components. Fig. 3 represents a material that loses its ductility by increasing the temperature. The brittle temperature range (BTR) is the critical range where the deformation rate surpasses the ductility curve and a solidification crack will occur. Based on this theory, if the strain during solidification reaches the minimum value (ε min) on the ductility curve, the system will reach its ductility limit, and a solidification crack will appear. Line A-D is the critical amount of deformation to cause a crack, while lines A-B and line A-C represent material thermal contraction and deformations by assuming that the material's ductility will be adequate to tolerate any strain during solidification.

Based on the explained theories, it can be concluded that hot cracking can be categorized as a result of either metallurgical or mechanical causes.

Comprehending solidification crack requires considering different factors determining the crack susceptibility. The highly complex

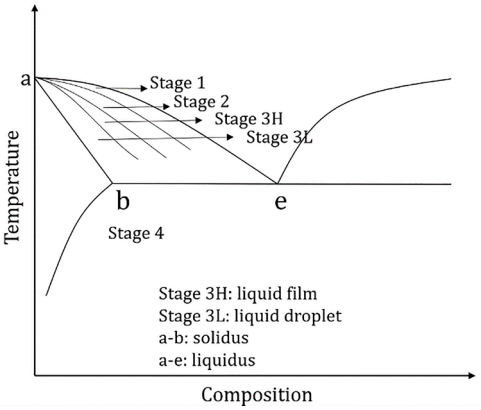

Fig. 2. Four stages of solidification based on the modified generalized theory (Matsuda et al., 1982).

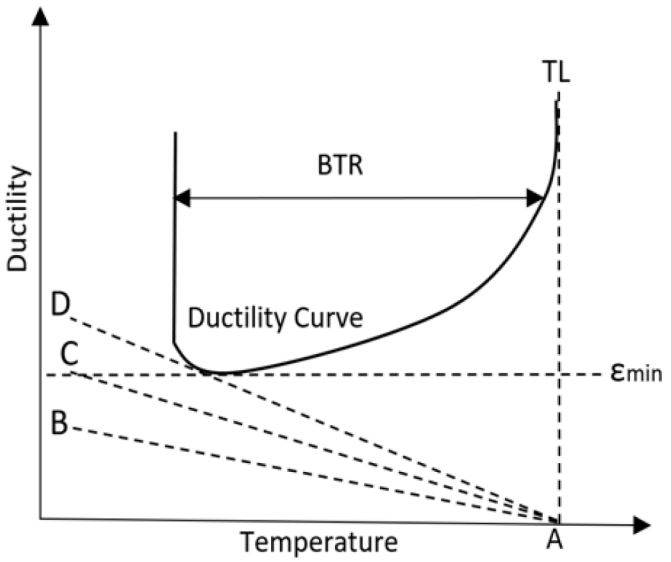

Fig. 3. Technological strength theory (Prokhorov and Prokhorov, 1971).

relationship between the mechanical and metallurgical factors accompanied the analysis of the solidification cracks with many difficulties. Thermal-metallurgical interactions control the solidification microstructure, and thermal-mechanical interactions govern the local and overall strains and stresses (Prokhorov 1971).

Fig. 4 depicts all the influential factors for SCS in laser welding. Having defined what is meant by the mechanism theories of solidification cracks. It has attempted to concentrate and provide a review relating to the role of the grain structure and chemical compositions on solidification cracks.

Understanding the effect of material, grain structure, and intermetallic phases in the solidification crack formation is critical. Sometimes due to the material properties, laser welding is quite challenging, and one should consider alternatives. Thus, this review focuses on the effect of grain size, shape, orientation of grains, chemical composition, composite segregation, and brittle intermetallic compounds to estimate the SCS.

The effect of grain structure on the solidification cracking

From a metallurgical aspect of view, in most cases, solidification cracks occur along grain boundaries and the role of grain boundary is very crucial (Liu and Kou, 2015; Kou, 2015). In addition, the microstructure of the weld has a remarkable contribution to the formation of the solidification cracks. Dendrites in the solidification process grow as columnar shapes under welding conditions. The interdendritic liquid creates residual films in the grain boundaries. The grain size and shape

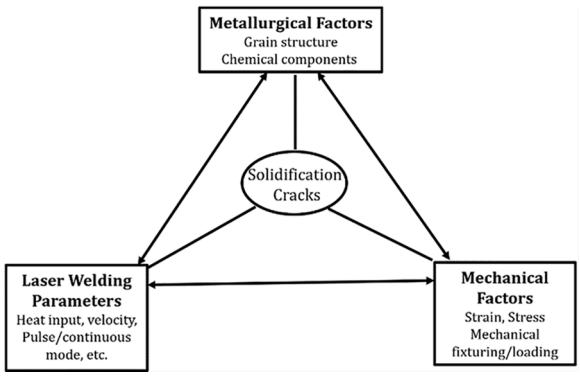

Fig. 4. Leading factors affecting solidification cracking.

directly affect the strain distribution on the grain boundaries of the mushy zone (Cross, 2005). In the columnar grains in which boundaries are aligned in the centerline, a weak channel for the residual liquid film leads to a full concentration of strain. It will boost the SCS (J. Campbell, 2003; Tang and Vollertsen, 2014). On the other side, fine equiaxed or globular grains have a substantial effect on reducing the SCS. Increasing grain boundaries by forming the equiaxed grains reduces the strain concentration in the solidification process. Indeed, due to the increased liquid permeability, this kind of grain can tolerate more deformations than a columnar one (Hunt, 1984).

Numerous studies have reported that the formation of shape and size of grains is determined by the solidification growth rate (R) and temperature gradient (G) (Kou, 2002a; Shao et al., 2019; Katayama, 2013). The solidification structure mode is determined by the G/R ratio, while its size is defined by the G*R (Kou, 2002a). Finer grains will ensure broader grain boundaries, which can lessen the unit strain per grain boundary length imposed by the solidification shrinkage of the low melting elements. The coarse grain, however, promotes the growth of microcracks, which diminishes the joint's strength (Sonar et al., 2021). Shinozaki et al. (2011) studied the effect of different grain sizes on inducing solidification cracks. They employed a U-type hot cracking test with the in-situ observation to estimate the strain rate of type 347 stainless steel with different grain sizes. To achieve various coarse sizes, specimens were held under heat treatment before laser welding. A measurement method is designed to quantify the crack susceptibility, and finally, a critical strain is achieved for forming solidification cracks (see Fig. 5 and Eq. (2)).

L_0 is the initial length, L_1 is the length for crack initiation, and ε_{cr} is the critical strain before solidification cracking. Based on the technological strength theory, the local critical strain was measured for various grain sizes from 69–112 μm. The Critical Strain Temperature (CST) ductility curve facilitates quantifying the solidification susceptibility. It is concluded that coarse grains are more susceptible to cracking than finer ones. Fig. 6 shows that the critical strain for the smallest grain, 69 μm, is higher than 210 μm.

$$\varepsilon_{cr} = \frac{L_1 - L_0}{L_1} \chi 100\% \quad (2)$$

Strategies to control grain structure and prevent solidification cracking

Grain refinement

Grain refinement as a solution to reduce crack susceptibility is considered a feasible and well-known technique (Mousavi et al., 1999). Significant grain refinement in the weld zone is achievable by inducing the nucleation of grains during solidification. It helps to change the coarse and columnar grains, which are the reasons for low critical strain and solidification cracks, to equiaxed and finer sizes (McCartney, 1989; Murty et al., 2002). Increasing the number of grain boundaries across the width of the weld leads to a reduction in SCS. Adding some alloying additives helps to control the cracks (Hagenlocher et al., 2019). For instance, Tibor™, which contains Titanium (Ti) and Boron (B) as the grain refiner, is added to the molten pool during the laser welding of AA5083 aluminum. Although the cooling rate is high, this refiner had a significant role in reducing grain size. It is reported that to achieve more equiaxed and finer grains in high-speed welding, more Tibor™ is required (Tang et al., 2011). Z. Tang et al. (Tang and Vollertsen, 2014) studied the mechanism of suppressing solidification crack by adding Ti and B as the grain refinement during laser welding. They based their studies on the effect of grain size on the main three factors of solidification theories. I. Dendrite network permeability, II. Mushy zone duration and III. Capillary pressure.

Fig. 7 shows the solidification zone's schematic while grains are refined in the laser welding process. The zone is divided into three parts. In the "melt" part, only liquid exists. The "slurry" part contains both

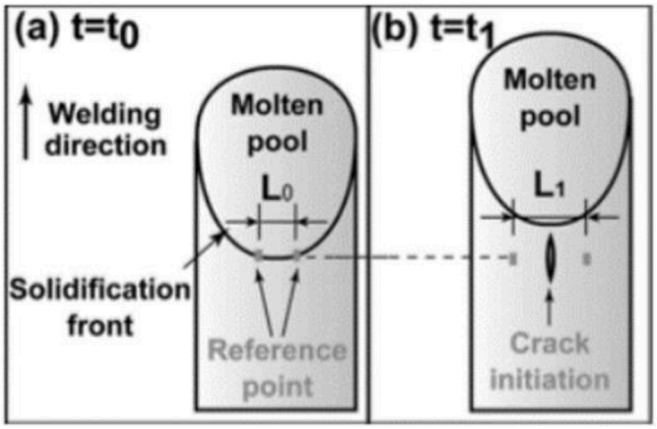

Fig. 5. Measurement method for the critical strain (Shinozaki et al., 2011).

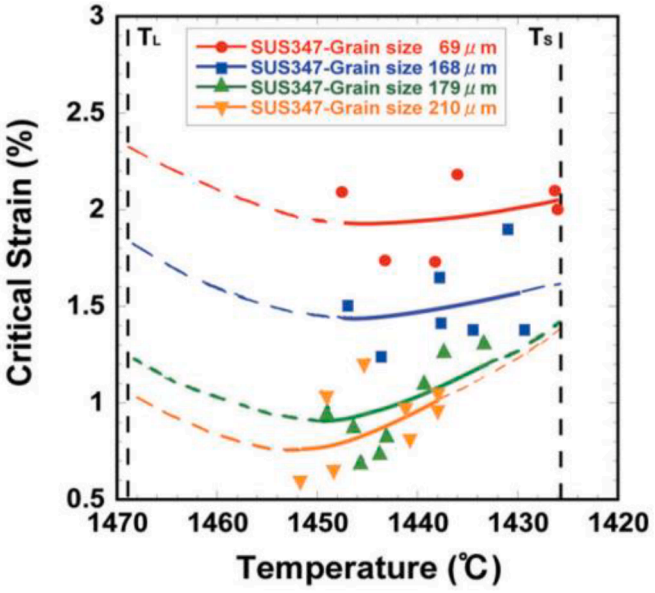

Fig. 6. Effect of grain size on the critical strain (Shinozaki et al., 2011).

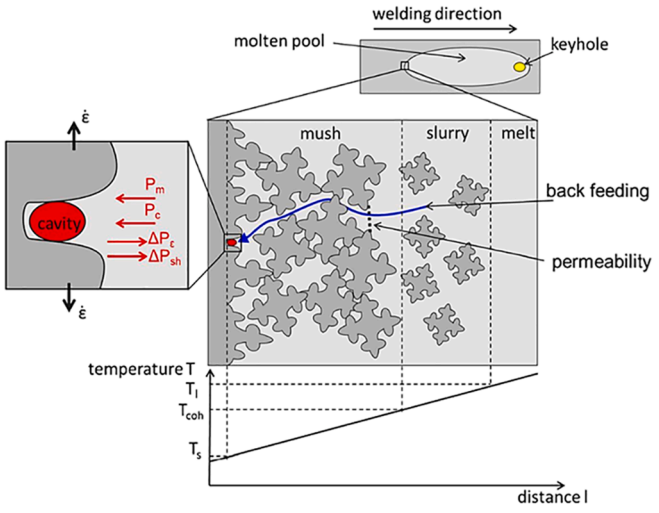

Fig. 7. Schematic of the weld pool in laser welding (Tang and Vollertsen, 2014).

solid and free-to-move liquid phases, and the "mush" part, where the dendrite arms are coalescent, generates a solid network. The temperature gradient in the lower part of the diagram shows that Ts is solidus temperature, Tl is liquidus temperature, and Tcoh is coherence temperature which separates slurry and mush parts. Pm is the static pressure and Pc is capillary pressure which is the reason for crack initiation resistance. $\dot{\varepsilon}$ shows the deformation rate due to the thermal contraction and solidification shrinkage. The pressure drop of ΔPε is due to thermal contraction and ΔPsh is because of solidification shrinkage. These two drop pressures are the cause of the creation pressure gradient between the melt and mush parts. The back-feeding liquid film is trying to fill the cavity to compensate for the pressure drop. However, this feeding depends on the permeability of dendrite networks and melt viscosity. If the back-feeding liquid does not reach the cavity, the crack will initiate from that area.

Studying the role of refining the grains in crack susceptibility by considering these three factors reported that if the aluminum grain size is 25 μm, the exposure of solidification crack will be minimized and 100% equiaxed grains are achievable. However, a saturated point shows very fine grains may even induce crack solidification. If the refinement process leads to a smaller size than 25 μm due to dendrite network permeability, SCS increases again (Tang and Vollertsen, 2014). (see Fig. 8.)

Laser welding with beam oscillation

The beam oscillation can refine the grains, without adding other material, to the finer and equiaxed grains (Li et al., 2020). The laser power of the entire radiation area can be dispersed by beam oscillation and make a molten turbulence pool (Li et al., 2020). Due to the driving impact of the beam oscillating, stress concentration will reduce, and it brings the possibility of appropriate solute migration. Laser oscillation welding increases the weld pool zone. Due to an extension of the laser radiation region, the average energy density may significantly reduce. Consequently, the growth of the cellular grains and dendrites is restricted by lower energy density. Furthermore, a wider weld pool width might induce complete solute diffusion at high temperatures and prolong the time it takes for the molten pool to solidify. The driving force generated by the oscillating laser can break dendrites and facilitate the movement of the solute. The entire diffusion of the solutes may significantly decrease the SCS. The behavior of the melt pool with and without beam oscillation is compared in Fig. 9 (Gao et al., 2022).

The weld pool shape as a function of the oscillation is also a sign of creating solidification cracks because it shows the strain distribution. Teardrop weld pool shape is more susceptible to cracking rather than an elliptical shape due to the concentration of the strain in the center line weld (Agarwal et al., 2019; Cross, 2005; Kou, 2021). Fig. 10 compares the teardrop shape with a high concentration of strain and an elliptical shape that distributes the strain along many grain boundaries in the center of the weld seam (Agarwal et al., 2019).

The circular oscillation helps to reduce the temperature gradient, and the sinusoidal pattern increases the solidification rate in the laser welding of AA6016 aluminum. Studies emphasized that oscillation patterns help obtain equiaxed crystals and enhance weldability (Hagenlocher et al., 2018).

More details of the oscillation and its effect on the grain size during fiber laser welding of AA6061-T6 aluminum alloy are reported by Wang et al. Three beam-oscillation, transverse, longitudinal, and circular, are compared to the linear laser welding. In Fig. 11, the microstructures of different solidification processes are presented. The molten pool without oscillation (a and b) shows the columnar grains. Due to the high-temperature gradient, dendrites along the weld centerline grow into axial grains in the heat flux direction. Transversely oscillation (c and d) forms turbulence in the melt pool, which can break the columnar dendrite network and develop the equiaxed grains. However, there are only a few equiaxed grains because the beam oscillation is in the front of the melt pool, and the turbulence is weak. The growth of equiaxed grains is increasing by longitudinally oscillating. It creates higher turbulence in the rear of the melting pool, which has more power to break the columnar grains. The creation of a wider melting pool because of the circular oscillation (g and h) leads to a slight temperature gradient. The constant circular melt flow enters the mushy zone and leads to high turbulence between dendrites. It can remelt the dendrite structures, and consequently, several broken dendrites will be made. At the same time, the circular melt flow pushes the fractured and partially melted grains into the molten pool and the mushy zone, creating new nuclei for the formation of equiaxed grains (Wang et al., 2016).

Kang et al., unlike other studies, concluded circular oscillation pattern may lead to a broader molten pool and higher SCS for Al 6014. However, the suppression of cracks by an infinite-shape pattern at 100 HZ and 3.5 m/min is feasible. The equiaxed grains at the center of the welding by this oscillation fluctuate and have different proportions (Kang et al., 2018).

Oscillation laser welding also can apply to other alloys like nickel-chromium-molybdenum (Ni-Cr-Mo) alloy. Reduction of a temperature gradient from 218.5 °C/mm to 73 °C/mm occurs while using 8-shape oscillation for the laser welding of the IN718 weld joint. The cooling rate also increased to 64.4% for the center of the weld pool and 111.9% for the edges. The ductility rate of specimens with oscillation is increased up to 20.3%. The fracture morphologies of the welded samples were also studied. The fracture surface of laser welded without oscillation has coarse grains and cracks along grain boundaries.

As a result of the refinement by oscillation with 50 and 150 Hz, larger grain boundaries are created. They can undergo plastic deformation, which is induced by the low melting of the liquid film of eutectic constituents and improves the distribution of the voids (Yan et al., 2022).

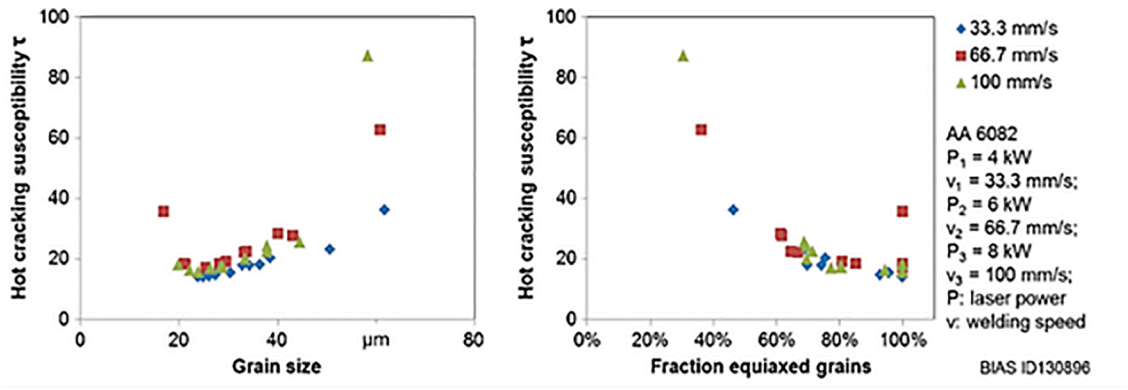

Fig. 8. Effect of grain size (left) and equiaxed grains(right) on SCS (Tang and Vollertsen, 2014).

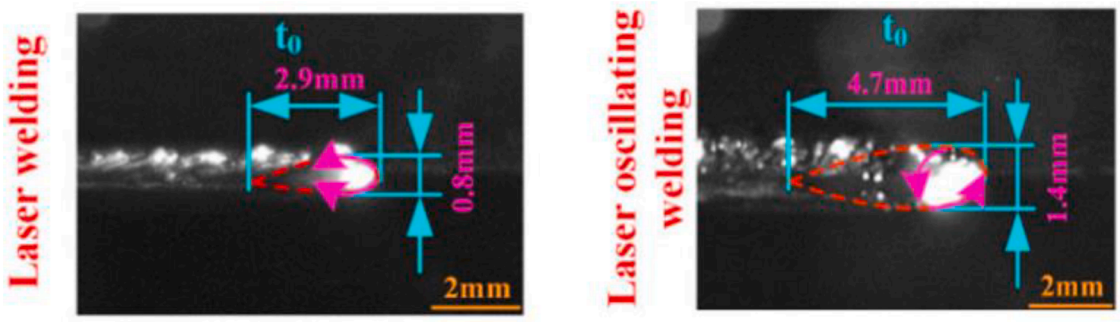

Fig. 9. Weld pool without (left) and with (right) oscillation (Gao et al., 2022).

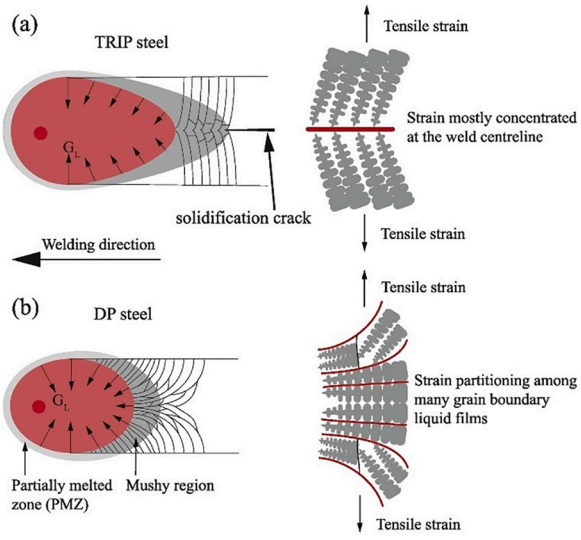

Fig. 10. Teardrop weld pool shape, b) Elliptical weld pool shape (Agarwal et al., 2019).

Vibration during laser beam welding

Alternative methods to achieve grain refinement and prevent solidification cracking defects include vibration. For instance, ultrasonic vibration and electromagnetic stirring during solidification. An electrodynamic shaker can be a source to excite the specimen while the laser welding process is ongoing. Results show that the solidification cracks are reduced by applying a vibration assistant method (Hagenlocher et al., 2019). Grain refinement is achievable through this technique for welding aluminum alloys. It causes the change of grain structure from columnar to equiaxed (Radel, 2018; Woizeschke et al., 2017).

In other investigations, the welding process uses ultrasonic vibration. It claims several benefits, including better material mixing, increased turbulence, higher heat generation, larger process windows, uniform grain growth, and improved mechanical properties (Kumar et al., 2017). In 1995, Kim et al. used an assistant ultrasonic vibration to improve and stabilize the molten pool in laser welding of aluminum-magnesium. A piezoelectric transducer with a 10 kHz resonant was used in this experiment. The vibration is considered an effective method that suppresses circumferential cracks and reduces more longitudinal cracks than laser welding without an ultrasonic assistant (Kim et al., 1995).

Ultrasonic-assisted weld solidification applied in welding of Inconel 718 alloy. Entirely elimination of solidification cracks was not possible due to inherent material properties. However, a high reduction in the comparison of welding without ultrasonic vibration is achieved. By ultrasonic sonotrode vibration, the dendrite arm in the solidification process reduces from 1256 to 89 μm, and crack sensitivity decreases from 47.5% to 13.3%. Cavitation implosion by ultrasonic leads to melting homogeneity, dispersing the solution, increasing homogenous and heterogenous nucleation, grain refinement, and SCS reduction (Thavamani et al., 2018).

Yao et al. supposed the effect of acoustic flow and cavitation as the reason for equiaxed crystal formation. Acoustic cavitation has the effect of raising the local melting point. The high pressure created by the cavitation bubbles explosion raises grain nucleation. In addition, the acoustic stream has the effect of increasing thermal convection, which is followed by thermal mixing brought on by latent heat and turbulence. This leads to the lowering of the temperature gradient. The ultrasonic cavitation bubbles significantly impact the molten pool, which explodes, dissolves, and flows away with the melt flow (Yao et al., 2022). The weld porosity is dramatically suppressed as a result of the cavitation, acoustic streaming, and thermal effects. The number of nucleation particles and refined grain is also increased by ultrasonic vibration during the crystallization phase of the weld pool. It improves the mechanical qualities of the welded joints (Lei et al., 2018).

Xu et al. (2016) applied Ultrasonic assisted welded-brazed magnesium-titanium Joints. They could reduce the size of the columnar α-Mg grains from 200 μm to 50 μm and achieve a high amount of equiaxed grains by an ultrasonic power of 1.2 kW.

Liu et al. (2022) proposed a newly ultrasonic-assisted laser welding called trailing ultrasonic-assisted laser welding (T-ULW). They compared the effect of ultrasonic vibration on the welding quality of SUS301L stainless steel.

Fig. 12.a shows three different modes of welding. Case A, ultrasonic sonotrode is fixed at a specified distance called (F-ULW). Case B is laser welding without ultrasonic vibration (LW), and Case C is laser welding while ultrasonic is moving with a specified distance in the same direction as welding. The molten pool fluid flow will change direction due to ultrasonic vibration, which will cause the fluid to stream more quickly downward. The wave of ultrasonic attenuates the weld pool. It will lead to a pressure gradient in the liquid from the weld pool's wall to its interior, which will subsequently intensify forced convection in the metal. Strong forced convection and disordered flow will make a welding pool with a more constant temperature distribution (Liu et al., 2022).

Monitoring the melt pool during laser welding shows that the solidification time can be prolonged under the T-ULW. Weld geometry studies reported that using F-ULW leads to pores and undercut defects in the weld. It is because the ultrasonic is fixed in the middle of the welding where the energy and vibration are concentrated. It leads to the viscous metal inside the melt pool that destroys the process severely, and finally, it makes some defects. Fig. 13 compares the effect of T-ULW and LW. It is observed that the columnar crystals are formed without ultrasonic, while in T-ULW, the structure is a more equiaxed crystal. Comparing T-ULW and F-ULW, both processes could refine the grains. However, the grain by T-ULW is finer and more uniformly distributed. In T-ULW, the cavitation from ultrasonic leads to the fracture of dendrites and grain

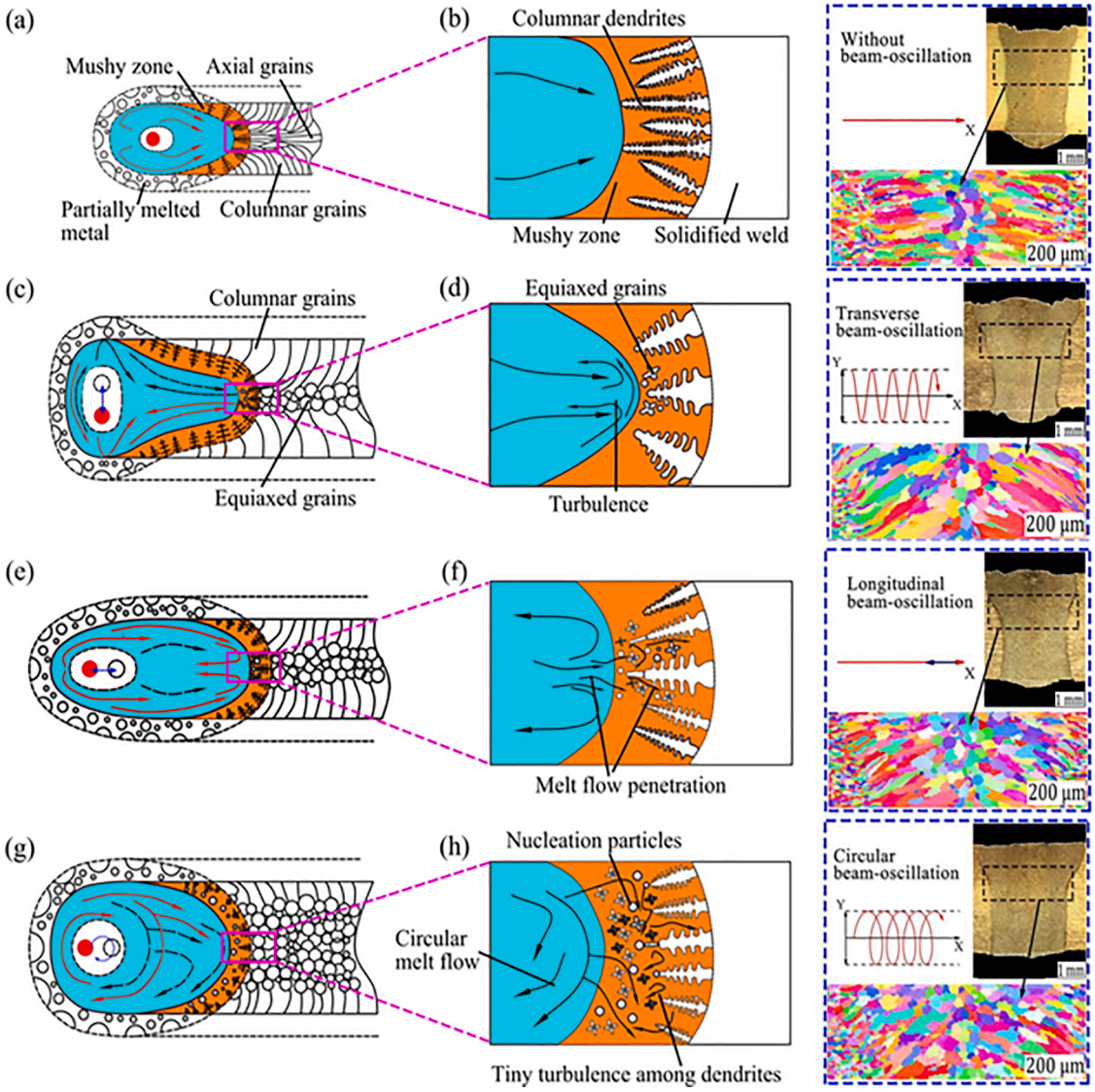

Fig. 11. Schematic of the weld pool, a,b) without oscillation, c,d) Transverse oscillation, e,f) Longitudinal oscillation, g,h) Circular oscillation (Wang et al., 2016).

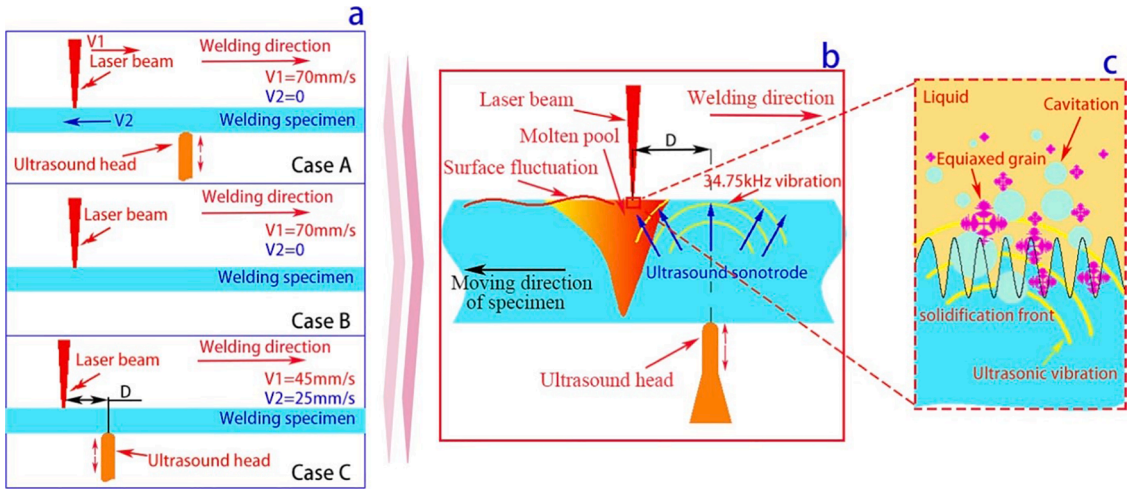

Fig. 12. Laser welding with ultrasonic vibration assisted a) welding modes b) schematic of ultrasonic vibration c) mechanism of vibration in the weld pool (Liu et al., 2022).

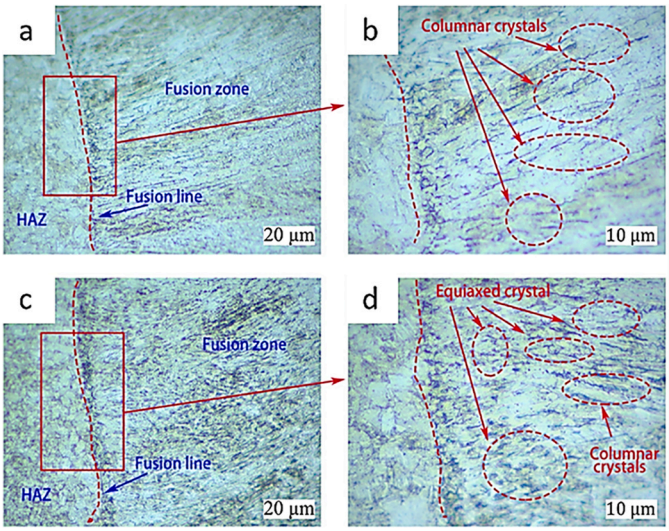

Fig. 13. Microstructure near to fusion zone, a, b) no ultrasonic assisted vibration (LW) c, d) trailing ultrasonic-assisted laser welding (T-ULW) (Liu et al., 2022).

boundaries. Thus, the equiaxed dendrite will grow and more grain boundaries will form (Liu et al., 2022).

Most studies concentrated on grain refinement to reduce welding defects like cracks. However, Liu et al. proposed ultrasonic vibration-assisted laser welding of dissimilar metals, Hastelloy C-276 and stainless steel 304, not only to refine the grain sizes but also to reduce the sizes of the precipitated phase. The cavitation effect raises the diffusion coefficient, and due to the shorter distances between elements in finer grains, the precipitated phases reduce from 2.15% to 0.62% by further ultrasonic vibration. 25 N ultrasonic pressing force and 13 mm distance from the laser welding position is enough to achieve excellent mechanical strength without cracks (Zhou et al., 2021).

Laser beam welding parameters

Local solidification rate and temperature gradient during welding are influenced by laser power, welding speed, continuous or pulsed mode, pre-heating, mechanical constraints, etc. Thus, they can affect the grain structure of the welded parts (Stritt et al., 2019). In addition, some restriction in welding is inevitable. For instance, laser welding of free-edge steel is investigated by Agarwal et al. (2018). In laser welding, there is a critical distance from the free edge that decreases the degree of self-restraint and increases the solidification crack susceptibility. However, controlling the laser parameters and reducing the heat input could decrease the critical distance from the free edge and suppress the solidification cracks of steel sheets.

Optimized process parameters facilitate the avoidance or reduction of solidification cracking in laser welding by affecting the grain structure and the transition from columnar to equiaxed grains by a drop in the cooling rate. Hekmatjou and Naffakh-Moosavy (2018) could achieve crack-free laser welding for 5456 aluminum alloy plates. The pre-heating is applied to reduce the cooling rate. They used the Nd: YAG pulsed laser with 20 Hz pulse frequency and 6 ms pulse duration, a velocity of 5 mm/s, and average power of 300 W to form an equiaxed microstructure that can spread the residual liquid in the grain boundary and control the solidification cracks. They proved that by increasing the pre-heating temperature from 25 °C to 300 °C at the fusion line, the G/R decreases, and the columnar grain structure would change to an equiaxed one. Fig. 14 compares welding without and with the preheating (room temperature and 300 °C).

Zhang et al. studied the relation between the fusion ratio and solidification cracks in the overlap welding of AA5754 and AA6013 aluminum. They observed the initiation of the crack from the fusion line and propagation along the columnar grain. Increasing the laser power could be an influential factor in reducing the crack susceptibility when AA6013 is on the top However, for the other stack up, and while AA5754 is on the top, less power is required to control crack formation. This is because the chemical composition affects the laser welding process and proves that each material requires specific parameters to reduce SCS (Zhang et al., 2015). These studies are followed on the effect of other

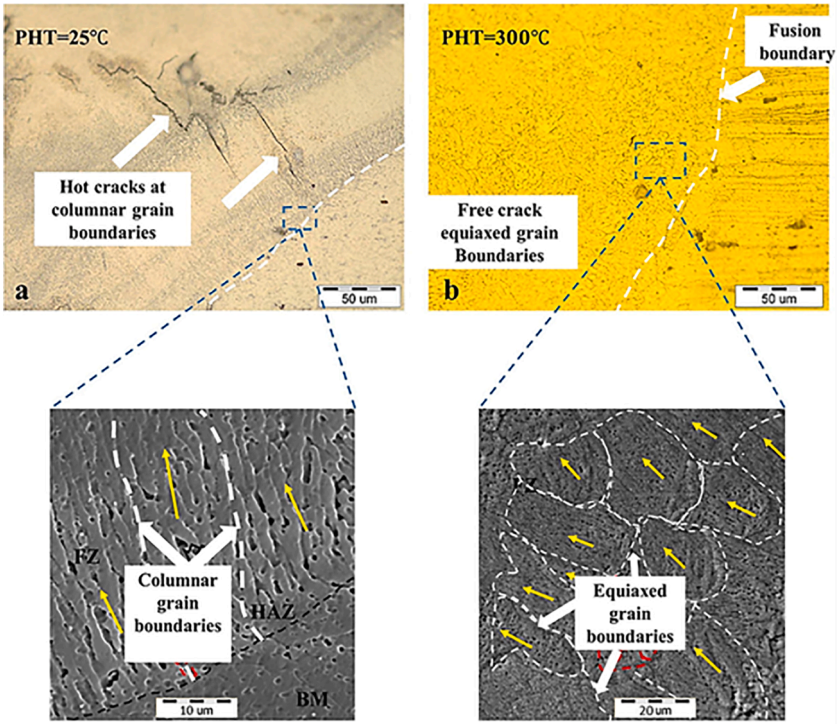

Fig. 14. a) Cellular structure without preheating, b) Equiaxed grains with preheating at 300 °C (Hekmatjou and Naffakh-Moosavy, 2018).

laser process parameters and their impact on the solidification cracking of the same materials. They considered a range of velocity and overlap for their experiments. There is a threshold relationship between the speed and the overlap width. To avoid cracks, when the overlap width was adjusted to 12, 10, 8, and 6 mm, the critical welding speed was, correspondingly, 3.0, 3.3, 3.9, and 4.5 m/min (Zhang et al., 2016).

The velocity is the factor affecting the temperature gradient and solidification and requires more investigation (Nguyen et al., 2020).

Wang et al. (2020) studied the effect of velocity on the solidification crack of three types of stainless steel with different grain structures. At 1.0 m/min velocity, SUS310 has more crack susceptibility because of the full austenite structure, while SUS304 appears with more ferrite structure and could have less solidification crack susceptibility. However, increasing the velocity to 2.0 m/min leads to grain refinement for SUS310 and decreasing the amount of ferrite for SUS304. Consequently, unlike the former speed, cracking susceptibility rises for SUS304 and reduces for SUS310.

The welding velocity affects the molten pool formation and also tension during solidification. In laser welding, a high velocity can be a reason for the high cooling rate. Since the time in a high cooling rate is not enough for the residual liquid to refill and heal the initiated crack, the crack will appear. Due to the high velocity in a low-duty cycle, the temperature gradient will be high, and the cooling rate will be faster; consequently, the SCS increases (Cicală et al., 2005; Milewski et al., 1993). Kadoi et al., (2013) used an in-situ observation of 310S stainless steel laser welding to determine the relationship between the velocity and critical strain for solidification cracks. They concluded that high-speed welding decreases the critical strain rate. This is because of the residual liquid film on the weld line center. However, these liquid films transfer to droplets at a lower velocity and stop the formation of solidification cracks (see Fig. 15).

Although some studies considered high-velocity welding as one of the influential factors of solidification cracks, however, it is a relative parameter. Material properties and other process parameters also affect the significance of velocity. For instance, high energy input is a determinative factor for the selection of welding speed. In the case of high energy input, increasing the welding speed directly impacts the grain structure. While at a relatively low speed, the grain structure in the fusion zone is columnar dendrite, due to the decreased heat input and corresponding greater cooling rate, the grain structure grew finer and more equiaxed in high-velocity laser welding (Palanivel et al., 2021). Experimental results of pulsed laser welding of austenitic stainless steel and copper are reported by Nguyen et al. (2020). The maximum power by the Nd: YAG pulsed laser is applied and the maximum temperature of 230 °C is achieved. The high laser peak power created a cooling rate that brought thermal stress to the welding zone. They observed that increasing the speed from 2 to 6 mm/s leads to 50 °C reductions, stabilizing the welding pool and minimizing the crack susceptibility.

Model simulation and analyzing the experimental results of solidification of aluminum alloy 6082 with various welding speeds show various grain structures. Due to the variant velocities, different thermal conditions lead to different grain structures. Mainly curved columnar grains are formed at two mm/s. The welding speed of 8.0 mm/s has curved columnar and some equiaxed grains. At the higher speed of 11.5 mm/s, the ratio of equiaxed grain size is higher than columnar. Fig. 16

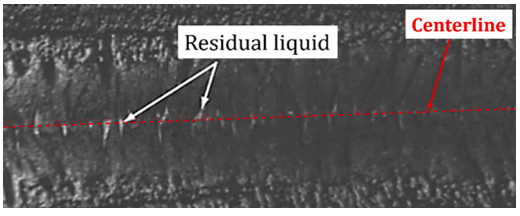

Fig. 15. Solidification In-situ observation at $t = 0.12$ s (Kadoi et al., 2013).

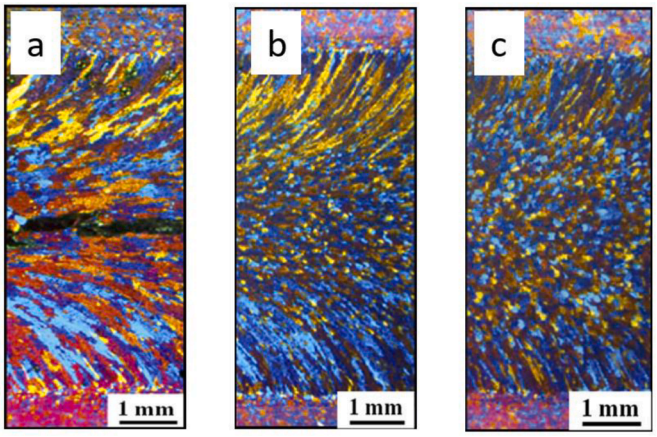

Fig. 16. a) Curved columnar grains at 2 mm/s, b) Curved columnar and equiaxed grains at 8 mm/s, and C) Curved columnar with a high proportion of equiaxed grain at 11.5 mm/s (Wei et al., 2016).

Compares the grain structures in the velocities of 2, 8 and 11.5 mm/s (Wei et al., 2016).

Zhang et al. (2021) studied the results of other researchers on the effect of laser pulse shaping on the microstructure and solidification cracking. They concluded that editing pulse shape could provide welding preheating and slow weld cooling. On the other hand, another heating source may also lead to the suppression of solidification cracks. Drezet et al. (2008) as for instance, used a double laser beam source to prevent solidification cracks on the welding of AA6016. While the CO_2 laser is used as the primary beam source, the Nd: YAG pulsed laser is considered the secondary heat source with a distance of $\delta_x = 3$ mm. the configuration of the two laser sources achieves an optimized thermal cycle. Due to its pulsed nature, the second laser source facilitates the transition from the columnar to equiaxed grains. This transition reduced grain sizes and strain localization. Due to the higher permeability in equiaxed grains, the liquid feeding increases in the mushy zone, and SCS is suppressed. Fig. 17. Shows a crack-free weld in a double laser beam source, while a solidification crack appeared with only a CO_2 laser beam source. The transient region begins the interaction of the second laser beam with the primary laser (0.1 s and 6 mm). The crack at the beginning of the interaction is unavoidable; however, the weld seam would be crack-free by passing the transient region.

Other process parameters, including beam focusing, beam quality, focal point, and laser power in laser welding of tempered steel, are studied by Schaefer et al. (2015) to understand their effect on creating solidification cracks. They observed that these parameters affect melt bath dynamics and cracks can be under control. For instance, If the beam quality is 2 mm.mrad at focal point to −3 mm, creates a transverse crack. X-ray analysis shows that reducing the focal point from −1.4 mm to −2.1 mm will affect the melt flow behavior. A focal position of −1.8 mm, few cracks will appear; however, increasing the focal point to −3 mm, creates a transverse crack. X-ray analysis shows that reducing the focal point from −1.4 mm to −2.1 mm will affect the melt flow behavior.

Schaefer et al. (2017) studied the process parameters of laser welding and concluded that velocity excessively impacts the solidification cracks. A new methodology, twin-spot optics, was applied to reduce the temperature gradient and influence the melt pool. They compared a) a single spot, b) a twin spot with a leading higher energy spot, and c) a trailing second laser spot with a specific distance to the first spot. It is concluded that tailoring the second spot close to the first spot at a welding speed of 2 m/min can hit 60% of the weld pool and change its geometry. The results show almost 0% cumulated crack length in the weld seam. Therefore, a reciprocal interaction exists between the weld pool geometry, melt flow eddies, and heat energy input. This makes it possible to entirely prevent hot cracks by impacting keyhole dynamics.

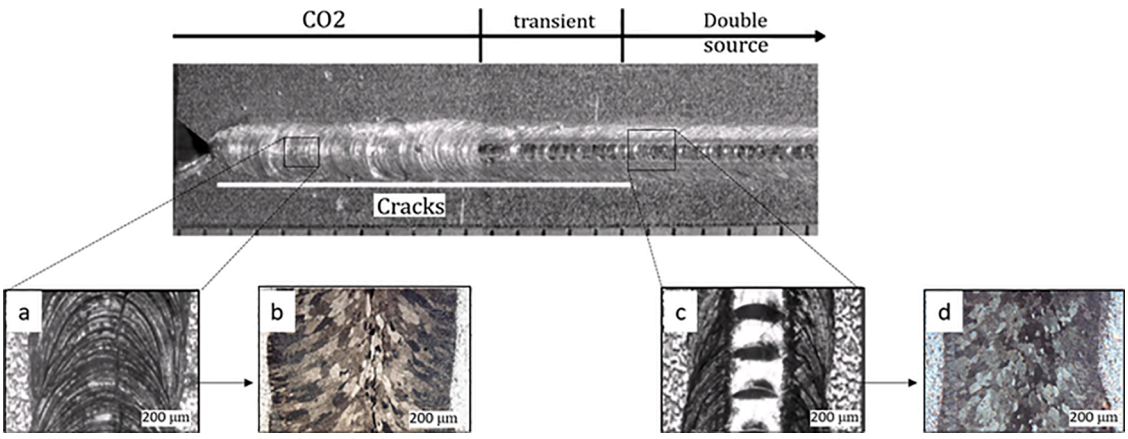

Fig. 17. a) Laser welding with CO2 laser, b) Solidification crack along columnar grains, c) double source welding, d) crack-free weld due to the higher permeability in the equiaxed grains (Drezet et al., 2008).

The effect of intermetallic compounds on the solidification cracking

The alloying elements are critical in the initiation and propagation of severe solidification cracking in carbon and low-alloy steels. The weld quality is affected by phase transformation, segregation of elements during solidification cracks. Even in very modest quantities, impurities induce solidification, and creation of intermetallic phases, inclusions, and precipitates brought on by alloy compositions (Huitron and Vuorinen, 2017; Agarwal et al., 2019; Palanivel et al., 2021; Azimzadegan and Akbari Mousavi, 2019). Taheri et al. (2020) studied the reasons for hot cracks on GTD-111 Nickel-based superalloy by pulsed laser welding. Observation of the fusion zone revealed that when the element distribution coefficient >1, W and Mo elements distribute in the interdendritic zone during the solidification and due to the strong reaction between the carbon and Ti, MC carbide forms in the interdendritic zone.

These carbides are considered the main factor for solidification cracks. The composition segregation within the grains might result in lattice distortion, decreasing the material's ductility and increasing the crack susceptibility (Gao et al., 2022). Gao et al. concluded that in laser welding of steel/Copper, the occurrence of solidification cracking is related to the inclusions and liquation of the ε phase, which weakens the cohesion between grains and reduces the plastic deformation.

The difference in the thermal expansion and contraction of the dissimilar materials, which causes cracking susceptibility, is the main challenge with laser welding of dissimilar materials. Welding materials with different properties brings a new mixture called intermetallic compounds (IMCs). IMCs are the results of involving two or more metals which are not soluble in solid-state during laser welding. Due to the low deformability of these compounds at room temperature, high residual stress during solidification is most probable. The difference in atomic size, electronegativity, crystal structure, and valency between dissimilar materials are the main factors of intermetallic formation. These detrimental compounds are unfavorable because they reduce the joint welded performance by increasing brittleness (Ponweiser et al., 2011). Dissimilar laser welding of Ti6Al4V/AA606, as an example, leads to residual stress and generation of IMCs, which are the sources of solidification cracks formation in the weld during the cooling and solidification (XUE et al., 2021). In another study by Hosseini et al. (2019) for welding of AA2021-T351, melting and coalescence of the spherical intermetallic of Al2CuM at the grain boundaries result in the nucleation of hot cracking.

This review aims to discuss and investigates in detail the effect of IMCs on solidification cracking. Hence focuses on two specific types of heterogeneous laser welding. Due to their inherent material properties, copper-aluminum and hard metal-steel laser welding are very challenging. The application of these materials in the industry is critical, requiring a precise analysis. For instance, Tungsten carbide (WC) is used in the production of cutting or drilling tools as the active part, while steel is used as the base and holder part (Costa et al., 2004). In the automotive battery industry, the Al-Cu joint can also reduce energy consumption and emission (Schmalen and Plapper, 2016). However, due to the physicochemical characteristic and the formation of IMCs, the mechanical strength reduces, leading to solidification cracks in some cases. Thus, due to the high importance of the application of these joints and their relatively higher sensitivity for forming IMCs, copper-aluminum and hard metal-steel are selected to comprehend the role of chemical compositions in SCS.

The following part of this paper moves on to describe in greater detail the types and effects of IMCs phases, and then preventive solutions for the reduction and distribution of IMCs will discuss.

The laser welding of hard metal and steel develops η phases, composite carbides like M_6C (Co_3W_3C), Fe_3W_3C, and $M_{12}C$ (Co_6W_6C), which reduce the mechanical strength and increase the SCS. The carbon in the hard metal tends to diffuse into the steel during the welding process, which causes a reduction in the carbon content of the hard metal. Considering the Phase diagram of WC—Co and WC-Fe alloys, the appearance of η phases seems inevitable due to the narrow zone of the (WC+γ) phase (Zhao et al., 2011).

Costa et al. studied the laser welding of hard metal-steel to reduce the porosity and crack defects. As hard metal is brittle and thermal shock sensitive, the weldability of this material is challenging. They examined high-power laser sources, such as CO_2 and Nd: YAG lasers. By optimizing the laser parameters and geometry of the weld, they could achieve crack-free welding in a relatively high percentage of cobalt as the hard metal binder. However, multiple intermetallic carbide compounds formed in the weld bead would be detrimental (Costa et al., 2003). Barbatti et al. reported the existence mixture of Fe_3W_3C and Fe_6W_6C as a fine network of the η phase in the steel side close to the fusion zone (Barbatti et al., 2003). These experiments are followed by Schiry and Plapper (2019), which employed a 400 W fiber laser for welding. Results show that a crack appeared due to the low vaporization of cobalt, complex IMCs, and intermediate phases. W_2C and $(WFe)_{12}C$ are observed as IMCs of tungsten carbide and steel. They lead to shear mechanical strength reduction and, in many cases, solidification cracks. Chen et al. (2013) observed cracks in the hard metal side because of the poor ductility of the weld and generated tensile stress. Fig. 18(a) depicts the crack in the HAZ of hard metal that extended to the weld joint. Fig. 18(b) shows two transition layers (I, II) with brittle compounds and WC in the hard metal interface. Zone I has more W elements due to the decomposition of WC and diffusion of the carbon atom. This led to a large formation of more eutectic microstructure. However, in Zone II,

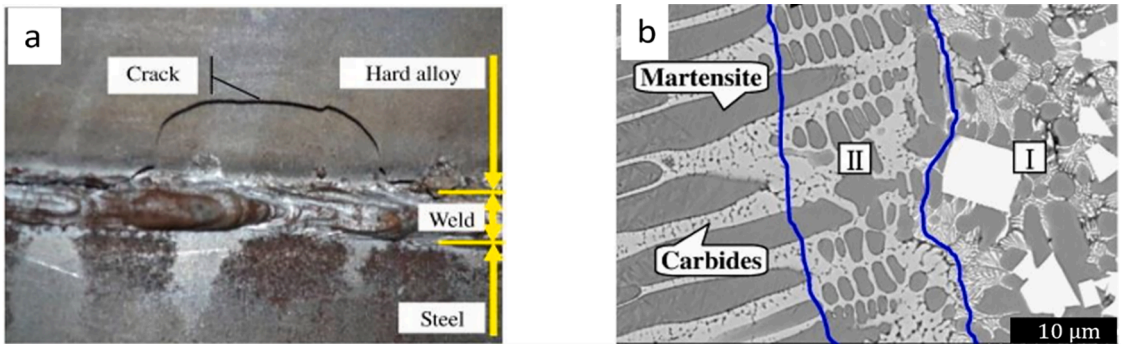

Fig. 18. a) Solidification cracks in hard tungsten carbide-steel joint b) WC and carbides in the hard metal interface(Chen et al., 2013).

the number of brittle compounds is reduced due to the lack of W elements. These observations revealed weak part of the joint is mainly because of the large number of carbides formed. Therefore, cracks would be inevitable in the weld or hard metal.

Yu et al. (2016) used the interlayer (Fe-Ni) to weld tungsten-carbide to steel by the fiber laser source. The butt-welded microstructure is studied and a predominant phase of α-WC and some IMCs like Fe_3W_3C and Co_6W_6C are formed in the fusion zone. In the HAZ of Tungsten carbide, there is α- WC (γ Fe, Ni) and a mixture of carbides, while in Steel HAZ, a martensite phase is observed. Hot cracks appeared in the fusion zone in the (γFe, Ni) matrix, along the grain boundaries, and cold cracks at the HAZ of Tungsten-carbide due to η-phase (mixed carbides) formed.

In laser welding of copper to aluminum, if the size of the IMCs is greater than 5 µm, a very brittle weld will be made following by high SCS (Braunovic, 2007). Mathivanan et al. proposed the existence of brittle intermetallic compounds because of the thermal nature of the process and very rapid cooling rate (Mathivanan and Plapper, 2019a). Dissimilar laser welding of Cu-Al is very challenging due to the difference in melting temperatures and density of materials. Al_3Cu_4, Al_2Cu (θ), Al_4Cu_9 (γ_1), and AlCu (η_2) are the intermetallic compounds that appear in the welding zone. Most cracks propagate in the interface between phase η2 and phase γ_1. These compounds cause brittleness and fracture (Schmalen et al., 2018).

Fig. 19 depicts the four main zones of aluminum-copper welding. The structure in the weld pool is a mixture of both materials. These four layers are Zone 1, a thin and uniform zone that consists of Cu_9Al_4 columnar grain. Zone 2 is the mixture of α-Al + θ-$CuAl_2$ and θ-$CuAl_2$, in which the amount of $CuAl_2$ is reduced by moving away from Cu to Al. Zone 3 is similar to the second zone but with a finer size. Zone 4 includes the dendrite microstructure due to the solidification growth. These observations and later analyses proved that the brittle θ-$CuAl_2$ phase has a detrimental impact on the strength of the joint (Zuo et al., 2014).

Dimatteo et al. investigated how the spot diameter affects the dissimilar laser lap welding of copper and aluminum. The findings demonstrated that a narrower spot diameter generated quality weld beads with greater control of penetration depth, less base metal mixing, and lower laser power needs. Because of the physical characteristics of copper, a wider laser spot requires more power to melt the material. In this case, the weld bead has large amounts of copper (over 50%) when full penetration occurs. As a result, the hardest and most brittle intermetallic compounds, (Al_3Cu_4) and (Al_4Cu_9) phases, will make. Fig. 20 shows the majority of the cracks developed along the intermetallic compounds on the copper side (Dimatteo et al., 2022).

Preventive solutions for the formation of IMCs

It is necessary to prevent or control the creation of hard and brittle intermetallic compounds to solidify crack-free joints. The preventive procedures for a dissimilar butt-joint weld are different. In the case of hard metal- steel, the laser beam spot should be on the steel side rather than on the hard metal. Schiry and Plapper (2019) defined a parameter called overlap Δy. Fig 21. shows the distance that the liquid steel could interact with hard metal during laser welding. It controls the formation of IMCs.

Fillers, the other solution, are considered to improve the mechanical strength of weld joints. However, it can also distribute the new IMCs in the weld seam (Yu et al., 2016). For instance, Zhao et al. (2011) used an interlayer with various Ni-Fe-C proportions in welding cemented carbide YG30 and Steel 1045. Three classes of η phases are observed. 1) η phase at HAZ with a similar size to WC. Its formation is related to the

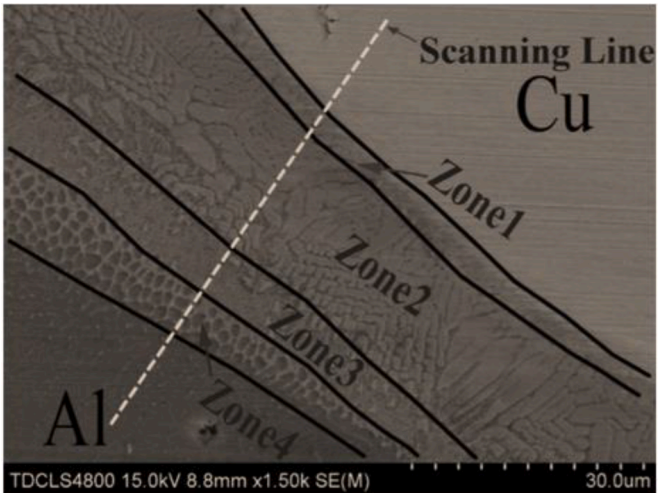

Fig. 19. Different zones in laser welding of Al-Cu (Zuo et al., 2014).

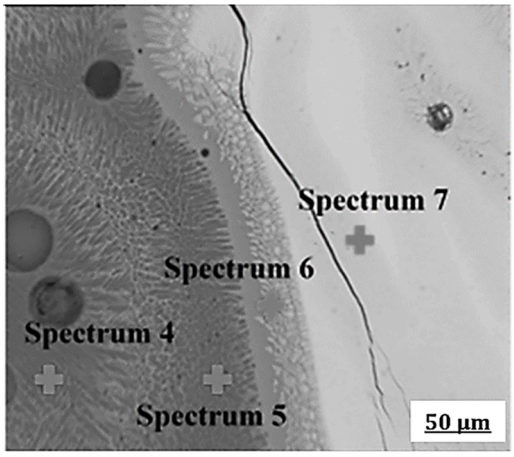

Fig. 20. Crack along the copper-rich intermetallic compounds(Dimatteo et al., 2022).

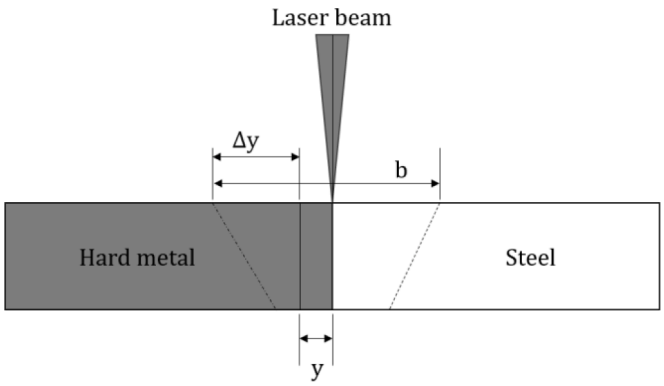

Fig. 21. Welding configuration (Schiry and Plapper, 2019).

interdiffusion between W, C, Fe, Co, and Ni in the solid-state γ phase, 2) Formed η phase between hard metal and weld zone by their nucleation in the melt pool, and 3) tiny η phase which precipitated from the oversaturated liquids during cooling. Optimizing the amount of filler, C, and Ni content controls the η phase. It is reported that the η phase can disappear by increasing the amount of C up to 0.6% and Ni up to 55%.

Chen et al. (2013) considered the three main reasons to use the Ni-Fe intermediate to improve the mechanical strength of the hard metal-steel joints and suppress crack formation. 1) Ni is an element that would not form IMCs with saturated C. 2) Ni relieves the welding stress and has high toughness. 3) due to the zero wetting angle between WC—Co and Ni, molten Ni can spread on the hard metal. Experiments confirmed no cracks in the weld or hard metal base while the Ni-Fe intermediate is used. Fig. 22 depicts the weld microstructure of the hard metal/ weld zone interface with Ni-Fe filler. They concluded that Ni-based filler could prevent the diffusion of the Fe element toward the hard metal. The solid solution with fewer carbides is the main weld microstructure close to the interface. It resulted in a crack-free joint.

Mai et al. (Dimatteo et al., 2022) reported that controlling the melting ratio of metals is crucial in butt welding of Cu-Al. They used a 350 W pulsed Nd: YAG laser to investigate laser welding without the use of filler materials. The laser beam offset technique has been proposed to prevent the development of intermetallic phases during butt laser welding of aluminum and copper. A crack-free weld is achieved by shifting 0.2 mm of the laser beam toward aluminum. However, increasing the welding velocity to 100 mm/min leads to solidification cracks.

Mai et al. (Mai and Spowage, 2004) reported that controlling the melting ratio of metals is crucial in butt welding of Cu-Al. They used a

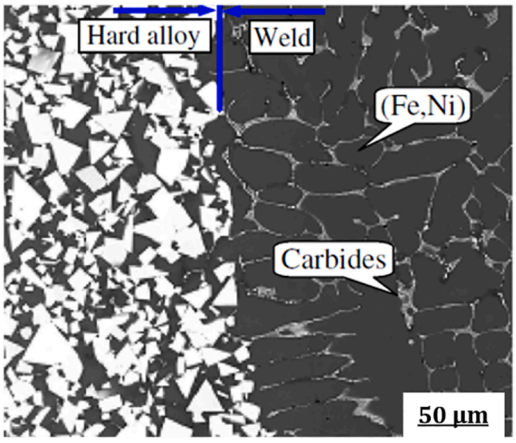

Fig. 22. Weld microstructure at the interface of hard metal with Ni-Fe intermediate (Chen et al., 2013).

350 W pulsed Nd: YAG laser to investigate laser welding without the use of filler materials. The laser beam offset technique has been proposed to prevent the development of intermetallic phases during butt laser welding of aluminum and copper. A crack-free weld is achieved by shifting 0.2 mm of the laser beam toward aluminum. However, increasing the welding velocity to 100 mm/min leads to solidification cracks.

Eliminating the detrimental compounds in the laser welding of Cu-Al may not be possible. However, it is a solution to avoid the accumulation of the intermetallic compound by distributing them throughout the fusion zone rather than the interface only. Infinite-shape beam oscillation is used in the laser welding process. A discontinuous weld seam that contains different degrees of compounds is formed. Therefore, welding of the Al-Cu is achieved by combining ductile and brittle intermetallic microstructure. Results show that infinite-shape beam oscillation brings higher ductility than linear welding and can control the propagation of cracks (Mathivanan and Plapper, 2019a).

Further studies completed and confirmed this experiment. They concluded that modifying the laser pulse shape by controlling brittle intermetallic compounds is possible. It can facilitate the distribution of the phases in a larger weld width. This can reduce the amount of porousness and degree of intermixing (Mathivanan and Plapper, 2019b).

Fetzer et al. (2016) considered using sinusoidal beam oscillation in the overlap laser welding of Cu-Al. The weld composition may be controlled by employing the right oscillation factors. Cracks appeared at a smaller amplitude of 0.25 mm due to inhomogeneous composition; however, by increasing the amplitude to 0.75 mm, less copper contributed to the fusion zone and a crack-free weld seam was achieved.

The use of interlayer, the adaptive filler, has been the subject of many investigations. Weigl et al. (2011) AlSi12 as the filler in the butt welding of Cu-Al. This filler achieves higher ductility because of its effect. In the molten pool, one reported viscosity reduction and turbulence increment. Therefore, a higher percentage of silicone helps improve ductility and reduce the formation of local IMCs.

Results and conclusions

Solidification cracking is a critical problem in the laser beam welding process. It significantly influences the industrial application of laser-welded parts. This paper reviewed the solidification crack mechanisms theories and discussed the effect of grain structure in laser welding of homogeneous materials and the critical role of IMCs on SCS for dissimilar materials. Then it proposed some strategies to suppress or minimize the solidification cracks. Based on the review, the paper summarizes the conclusions:

1. Based on mechanism theories, the solidification crack often occurs along grain boundaries due to the appearance of the residual liquid film in the solidification process. In the coherent zone and during the solidification process, when there is a thin residual liquid film between the grain boundaries, the grain coalescence flows according to the attraction and repulsion forces. If the energy at the grain boundary is less than twice that at the solid-liquid contact when dendrites reach a specific interaction distance, the liquid film becomes erratic, and grains merge. If not, the liquid film is stable and keeps the dendrites apart. Due to the residual liquid film at the grain boundaries during solidification and reaching the critical temperature, solidification cracks appear on the fusion zone.
2. The weld's microstructure has a notable contribution to the development of solidification cracks. The grain size and shape directly impact the strain distribution on the grain boundaries of the mushy zone. The strain concentration in the centerline of the weld seam with columnar grains is higher than equiaxed grains, and it can lead to solidification cracks. A weak path for the residual liquid film causes a complete concentration of strain in the columnar grains whose borders are aligned in the centerline. However, Fine,

equiaxed, or globular grains significantly lower the SCS. The formation of equiaxed grains increases grain boundaries and decreases strain concentration during solidification. Indeed, the high permeability of liquid through more grain boundaries in equiaxed grains helps to tolerate more deformation.

3. Grain refinement with vibration-assisted laser welding provides several advantages, such as more significant material mixing, enhanced turbulence, higher heat generation, bigger process windows, consistent grain development, and low SCS. A welding pool with a more uniform temperature distribution will result from strong forced convection and disordered flow due to ultrasonic attenuation. During the solidification phase, ultrasonic vibration multiplies the number of nucleation particles and refined grain. For instance, dendrites and grain boundaries in T-ULW are broken due to ultrasonic cavitation. The equiaxed grains will increase, and additional grain boundaries without solidification cracks will result.
4. Oscillating laser welding can spread the radiation area and create a molten turbulence pool. Dendrites can be broken by the oscillating laser's driving force, making it easier for the solute to move. Circular oscillation can make a wider melting pool than laser welding without oscillation and longitudinal and transverse oscillations. High turbulence occurs between dendrites because of the continual circular melt flow crossing the mushy zone. Circular melt flow facilitates the formation of equiaxed grains by pushing the broken dendrites to the melt zone and creating nuclei. Beam oscillation achieves a weld with low SCS by controlling the growth of cellular grains and transforming them into equiaxed grains.
5. In addition implementing double laser sources, like other methods, such as adding refiner material, pulsed laser welding, pre-heat treatment and optimizing laser parameters, changes the columnar to equiaxed grains and leads to SCS reduction in welding of various alloys.
6. Laser welding of dissimilar materials may lead to the formation of IMCs that affect the mechanical strength of the joint and consider one of the main reasons for the solidification cracks. The leading causes of intermetallic formation include differences in atomic size, electronegativity, crystal structure, and valency between different materials. IMCs have poor ductility and a detrimental impact on the weld seam because they can be the main reason for hot cracking during solidification. Laser welding with beam oscillation, adding fillers, and adjusting the laser beam spot are considered the preventive procedure for solidification cracks. However, more studies can be helpful, like the effect of heat treatment and ultrasonic-assisted laser welding on suppression or minimizing the brittle compounds in the welding of dissimilar materials.

Declaration of Competing Interest

The authors declare that they have no known competing financial interests or personal relationships that could have appeared to influence the work reported in this paper.

Data availability

No data was used for the research described in the article.

Acknowledgements

The presented work is based on the ''Developing and Online Monitoring of Laser Welding Between Hard metal and Steel Based on Artificial Neural Network Feedback'' project (AFR-PPP grant, Reference 16663291). The authors would like to thank the support of the Luxembourg National Research Fund (FNR) and acknowledge Ceratizit Luxembourg as the project's industrial partner.

References

Agarwal, G., et al., 2018. Study of solidification cracking susceptibility during laser welding in an advanced high strength automotive steel. Metals (Basel) 8 (9). https://doi.org/10.3390/met8090673. Available at.

Agarwal, G., et al., 2019. Evaluation of solidification cracking susceptibility during laser welding in advanced high strength automotive steels. Mater. Des. 183 https://doi.org/10.1016/j.matdes.2019.108104. Available at.

Amne Elahi, M., et al., 2021. Failure mechanism analysis based on laser-based surface treatments for aluminum-polyamide laser joining. J. Mater. Proces. Technol. 298 https://doi.org/10.1016/j.jmatprotec.2021.117318. Available at.

Amne Elahi, M., Plapper, P, 2019. Dissimilar laser micro-welding of nickel wire to CuSn6 bronze terminal. Trans. Indian Inst. Metals 72 (1), 27–34. https://doi.org/10.1007/s12666-018-1457-y. Available at.

Aplett WR, P.W., 1954. Factors which influence weld hot cracking. Welding J. (N.Y.) 33, 83–90. Available at. https://www.osti.gov/biblio/4389407.

Azimzadegan, T., Akbari Mousavi, S.A.A., 2019. Investigation of the occurrence of hot cracking in pulsed Nd-YAG laser welding of Hastelloy-X by numerical and microstructure studies. J. Manuf. Process. 44, 226–240. https://doi.org/10.1016/j.jmapro.2019.06.005. Available at.

Barbatti. C. et al. (2003) Determination of phases and residual stresses in laser beam welded joints of cemented carbide to steel.

Borland, J.C., 1960. Generalized theory of super-solidus cracking in welds (and castings). Br. Weld. J 508–512.

Braunovic, M., 2007. Reliability of power connections. J. Zhejiang Univ. Sci. 8 (3), 343–356. https://doi.org/10.1631/jzus.2007.A0343. Available at.

Campbell, J., 2003. Castings. Available at, 2nd Edition. https://doi.org/10.1016/B978-075064790-8/50016-4.

Chen, G., et al., 2013. Electron beam welding-brazing of hard alloy to steel with Ni-Fe intermediate. Int. J. Refractory Metals Hard Mater. 58–63. https://doi.org/10.1016/j.ijrmhm.2013.03.002. Available at.

Cicală, E., et al., 2005. Hot cracking in Al-Mg-Si alloy laser welding - operating parameters and their effects. Mater. Sci. Eng. A 395 (1–2), 1–9. https://doi.org/10.1016/j.msea.2004.11.026. Available at.

Costa, A., Quintino, L., Miranda, R.M., 2004. Microstructural aspects of laser dissimilar welds of hard metals to steels. J. Laser Appl. 16 (4), 206–211. https://doi.org/10.2351/1.1809635. Available at.

Costa, A.P., Quintino, L., Greitmann, M., 2003. Laser beam welding hard metals to steel. J. Mater. Process. Technol. 141 (2), 163–173. https://doi.org/10.1016/S0924-0136(02)00954-8. Available at.

Cross, C.E., 2005. On the origin of weld solidification cracking. Hot Cracking Phenomena in Welds. Springer-Verlag, Berlin/Heidelberg, pp. 3–18. https://doi.org/10.1007/3-540-27460-X_1. Available at.

Dimatteo, V., et al., 2022. Experimental investigation on the effect of spot diameter on continuous-wave laser welding of copper and aluminum thin sheets for battery manufacturing. Opt. Laser Technol. 145 https://doi.org/10.1016/j.optlastec.2021.107495. Available at.

Drezet, J.-.M. et al. (2008) Crack-free aluminium alloy welds using a twin laser process.

Fetzer, F., et al., 2016. Fine-tuned remote laser welding of aluminum to copper with local beam oscillation. Physics Procedia. Elsevier B.V., pp. 455–462. https://doi.org/10.1016/j.phpro.2016.08.047. Available at.

Gao, Z., et al., 2022. Formation mechanism and control of solidification cracking in laser-welded joints of steel/copper dissimilar metals. Metals (Basel) 12 (7), 1147. https://doi.org/10.3390/met12071147. Available at.

Hagenlocher, C., et al., 2018. Optimization of the solidification conditions by means of beam oscillation during laser beam welding of aluminum. Mater. Des. 160, 1178–1185. https://doi.org/10.1016/j.matdes.2018.11.009. Available at.

Hagenlocher, C., et al., 2019. Reduction of the hot cracking susceptibility of laser beam welds in AlMgSi alloys by increasing the number of grain boundaries. Sci. Technol. Weld. Join. 24 (4), 313–319. https://doi.org/10.1080/13621718.2018.1534775. Available at.

Han, C., et al., 2021. Multiphase-field simulation of grain coalescence behavior and its effects on solidification cracking susceptibility during welding of Al-Cu alloys. Mater. Des. 211 https://doi.org/10.1016/j.matdes.2021.110146. Available at.

Hekmatjou, H., Naffakh-Moosavy, H., 2018. Hot cracking in pulsed Nd:YAG laser welding of AA5456. Opt. Laser Technol. 103, 22–32. https://doi.org/10.1016/j.optlastec.2018.01.020. Available at.

Hosseini, S.A., et al., 2019. Elimination of hot cracking in the electron beam welding of AA2024-T351 by controlling the welding speed and heat input. J. Manuf. Process. 46, 147–158. https://doi.org/10.1016/j.jmapro.2019.09.003. Available at.

Huitron, R.M.P., Vuorinen, E., 2017. Hot cracking of structural steel during laser welding. In: IOP Conference Series: Materials Science and Engineering. Institute of Physics Publishing. https://doi.org/10.1088/1757-899X/258/1/012005. Available at.

Hunt, J.D., 1984. Steady state columnar and equiaxed growth of dendrites and eutectic. Mater. Sci. Eng. R. Rep. 65 (1), 75–83. https://doi.org/10.1016/0025-5416(84)90201-5. Available at.

Jonathan Dantzig, M.R. (2007) Solidification: 2nd Edition, Revised & Expanded. Available at: https://books.google.lu/books?id=k1Q-DgAAQBAJ.

Kadoi, K., et al., 2013. The effect of welding conditions on solidification cracking susceptibility of type 310S stainless steel during laser welding using an in-situ observation technique. Weld. World 57 (3), 383–390. https://doi.org/10.1007/s40194-013-0023-9. Available at.

Kang, M., Han, H.N., Kim, C., 2018. Microstructure and solidification crack susceptibility of Al 6014 molten alloy subjected to a spatially oscillated laser beam. Materials (Basel) 11 (4). https://doi.org/10.3390/MA11040648. Available at.

Katayama, S., 2013. Defect formation mechanisms and preventive procedures in laser welding. Handbook of Laser Welding Technologies. Elsevier Inc., pp. 332–373. https://doi.org/10.1533/9780857098771.2.332. Available at.

Katayama, S., 2020. Fundamentals and Details of Laser Welding. Springer Singapore, Singapore. https://doi.org/10.1007/978-981-15-7933-2. Topics in Mining, Metallurgy and Materials EngineeringAvailable at.

Katayama. S. (2013) 'Handbook of Laser Welding Technologies'. Available at: https://www.sciencedirect.com/book/9780857092649/handbook-of-laser-welding-technologies.

Kim, J.S., Watanabe, T., Yoshida, Y., 1995. Ultrasonic vibration aided laser welding of Al alloys: improvement of laser welding-quality. J. Laser Appl. 7 (1), 38–46. https://doi.org/10.2351/1.4745370. Available at.

Kou, S., 2002. Welding Metallurgy. John Wiley & Sons, Inc, Hoboken, NJ, USA. https://doi.org/10.1002/0471434027. Available at.

Kou, S., 2015. A criterion for cracking during solidification. Acta Mater. 88, 366–374. https://doi.org/10.1016/j.actamat.2015.01.034. Available at.

Kou, S., 2021. Solidification cracking susceptibility associated with a teardrop-shaped weld pool. Sci. Technol. Weld. Joining 26 (4), 341–347. https://doi.org/10.1080/13621718.2021.1910179. Available at.

Kumar, S., et al., 2017. Application of ultrasonic vibrations in welding and metal processing: a status review. J. Manuf. Process. 295–322. https://doi.org/10.1016/j.jmapro.2017.02.027. Available at.

Lei, Z., et al., 2018. Melt flow and grain refining in ultrasonic vibration assisted laser welding process of AZ31B magnesium alloy. Opt. Laser Technol. 108, 409–417. https://doi.org/10.1016/j.optlastec.2018.07.015. Available at.

Li, J., et al., 2020a. Melt flow and microstructural characteristics in beam oscillation superimposed laser welding of 304 stainless steel. J. Manuf. Process. 50, 629–637. https://doi.org/10.1016/j.jmapro.2019.12.053. Available at.

Li, S., Mi, G., Wang, C., 2020b. A study on laser beam oscillating welding characteristics for the 5083 aluminum alloy: morphology, microstructure and mechanical properties. J. Manuf. Process. 53, 12–20. https://doi.org/10.1016/j.jmapro.2020.01.018. Available at.

Lippold, J.C., 2015. Welding Metallurgy and Weldability. John Wiley & Sons, Inc. Available at, Hoboken, NJ. https://doi.org/10.1002/9781118960332.

Liu, J., Kou, S., 2015. Effect of diffusion on susceptibility to cracking during solidification. Acta Mater. 100, 359–368. https://doi.org/10.1016/j.actamat.2015.08.064. Available at.

Liu, Z., et al., 2022. Microstructure evolution and mechanical properties of SUS301L stainless steel sheet welded joint in ultrasonic vibration assisted laser welding. Opt. Laser Technol. 153 https://doi.org/10.1016/j.optlastec.2022.108193. Available at.

Mai, T.A., Spowage, A.C., 2004. Characterisation of dissimilar joints in laser welding of steel-kovar, copper-steel and copper-aluminium. Mater. Sci. Eng. A 374 (1–2), 224–233. https://doi.org/10.1016/j.msea.2004.02.025. Available at.

Manitsas, D., Andersson, J., 2018. Hot cracking mechanisms in welding metallurgy: a review of theoretical approaches. In: MATEC Web of Conferences. EDP Sciences. https://doi.org/10.1051/matecconf/201818803018. Available at.

Mathivanan, K. and Plapper, P. (2019a) Laser overlap joining from copper to aluminum and analysis of failure zone. Available at: http://hdl.handle.net/10993/40126.

Mathivanan, K., Plapper, P., 2019b. Laser welding of dissimilar copper and aluminum sheets by shaping the laser pulses. Procedia Manufacturing. Elsevier B.V., pp. 154–162. https://doi.org/10.1016/j.promfg.2019.08.021. Available at.

Matsuda, Fukuhisa, Nakagawa, Hiroji, Sorada, Kazuhiko, 1982. Dynamic observation of solidification and solidification cracking during welding with optical microscope (I) : solidification front and behavior of cracking(Materials, metallurgy \& weldability). Trans. JWRI 11, 67–77.

McCartney, D.G., 1989. Grain refining of aluminium and its alloys using inoculants. Int. Mater. Rev. 34 (1), 247–260. https://doi.org/10.1179/imr.1989.34.1.247. Available at.

Milewski, J.O., Lewis, G.K. and Wittig, J.E. (1993) Microstructural evaluation of low and high duty cycle Nd:YAG laser beam welds in 2024-T3 aluminum changes in weld microstructure due to an increased duty cycle produced acceptable laser weld morphology in a hot-tear-sensitive alloy. Available at: https://www.osti.gov/biblio/6354358.

Mousavi, M.G., Cross, C.E., Grong, Ø., 1999. Effect of scandium and titanium–boron on grain refinement and hot cracking of aluminium alloy 7108. Sci. Technol. Weld. Joining 4 (6), 381–388. https://doi.org/10.1179/136217199101538030. Available at.

Murty, B.S., Kori, S.A., Chakraborty, M., 2002. Grain refinement of aluminium and its alloys by heterogeneous nucleation and alloying. Int. Mater. Rev. 47 (1), 3–29. https://doi.org/10.1179/095066001225001049. Available at.

Nguyen, Q., et al., 2020. Experimental investigation of temperature field and fusion zone microstructure in dissimilar pulsed laser welding of austenitic stainless steel and copper. J. Manuf. Process. 56, 206–215. https://doi.org/10.1016/j.jmapro.2020.03.037. Available at.

P.rokhorov, N.N., P.rokhorov, N.N., 1971. Fundamentals of the theory for technological strength of metals while crystallising during welding. Trans. Japan Weld. Soc. 2, 205–213.

Palanivel, R., et al., 2021. Effect of Nd:YAG laser welding on microstructure and mechanical properties of Incoloy alloy 800. Opt. Laser Technol. 140. https://doi.org/10.1016/j.optlastec.2021.107039. Available at.

Ponweiser, N., Lengauer, C.L., Richter, K.W., 2011. Re-investigation of phase equilibria in the system Al-Cu and structural analysis of the high-temperature phase η1-Al 1-δCu. Intermetallics 19 (11), 1737–1746. https://doi.org/10.1016/j.intermet.2011.07.007. Available at.

Pumphrey, W., 1948. A consideration of the nature of brittleness at temperatures above the solidus in castings and welds in aluminium alloys. J. Inst. Metals 230–254.

Radel, T., 2018. Mechanical manipulation of solidification during laser beam welding of aluminum. Weld. World 62 (1), 29–38. https://doi.org/10.1007/s40194-017-0530-1. Available at.

Schaefer, M. et al. (2015) Analysing hot crack formation in laser welding of tempered steel. Available at: https://www.wlt.de/lim/Proceedings2015/Stick/PDF/Contribution148_final.pdf.

Schaefer, M., et al., 2017. Hot cracking during laser welding of steel: influence of the welding parameters and prevention of cracks. In: High-Power Laser Materials Processing: Applications, Diagnostics, and Systems VI. SPIE, 100970E. https://doi.org/10.1117/12.2254424 pAvailable at.

Schiry, M. and Plapper, P. (2019) Elucidation of influencing parameters of the laser butt welding process of dissimilar steel to tungsten alloy sheets. Available at: http://hdl.handle.net/10993/39387.

Schmalen, P., et al., 2018. Composition and phases in laser welded Al-Cu joints by synchrotron x-ray microdiffraction. Procedia CIRP. Elsevier B.V., pp. 27–32. https://doi.org/10.1016/j.procir.2018.08.006. Available at.

Schmalen, P., Plapper, P., 2016. Evaluation of laser braze-welded dissimilar Al-Cu joints. Physics Procedia. Elsevier B.V., pp. 506–514. https://doi.org/10.1016/j.phpro.2016.08.052. Available at.

Shankar, V., Devletian, J.H., 2005. Solidification cracking in low alloy steel welds. Sci. Technol. Weld. Joining 10 (2), 236–243. https://doi.org/10.1179/174329305X39266. Available at.

Shao, J., et al., 2019. Grain size evolution under different cooling rate in laser additive manufacturing of superalloy. Opt. Laser Technol. 119 https://doi.org/10.1016/j.optlastec.2019.105662. Available at.

Shinozaki, K., et al., 2011. Effect of grain size on solidification cracking susceptibility of type 347 stainless steel during laser welding. Yosetsu Gakkai Ronbunshu 29 (3), 90s–94s. https://doi.org/10.2207/qjjws.29.90s. Available at.

Sonar, T., et al., 2021. An overview on welding of Inconel 718 alloy - effect of welding processes on microstructural evolution and mechanical properties of joints. Materials Characterization. Elsevier Inc. https://doi.org/10.1016/j.matchar.2021.110997. Available at.

Stritt, P. et al. (2019) 'The effect of laser welding parameters on the grain structure distribution in the resultant weld', in. Laser Institute of America, p. 1201. Available at: https://doi.org/10.2351/1.5119065.

Taheri, M., Halvaee, A., Kashani-Bozorg, S.F., 2020. Hot cracking of GTD-111 nickel-based superalloy welded by pulsed Nd:YAG laser. Metallogr., Microstruct., Anal. 9 (1), 16–32. https://doi.org/10.1007/s13632-019-00602-8. Available at.

Tang, Z., Seefeld, T., Vollertsen, F., 2011. Grain refinement by laser welding of AA 5083 with addition of Ti/B. Physics Procedia. Elsevier B.V., pp. 123–133. https://doi.org/10.1016/j.phpro.2011.03.016. Available at.

Tang, Z., Vollertsen, F., 2014. Influence of grain refinement on hot cracking in laser welding of aluminum. Weld. World 58 (3), 355–366. https://doi.org/10.1007/s40194-014-0121-3. Available at.

Thavamani, R., et al., 2018. Mitigation of hot cracking in Inconel 718 superalloy by ultrasonic vibration during gas tungsten arc welding. J. Alloys Compd. 740, 870–878. https://doi.org/10.1016/j.jallcom.2017.12.295. Available at.

Wallerstein, D., et al., 2021. Recent developments in laser welding of aluminum alloys to steel. Metals (Basel) 11 (4), 622. https://doi.org/10.3390/met11040622. Available at.

Wang, J., et al., 2015. Statistical analysis of process parameters to eliminate hot cracking of fiber laser welded aluminum alloy. Opt. Laser Technol. 66, 15–21. https://doi.org/10.1016/j.optlastec.2014.08.009. Available at.

Wang, L., et al., 2016. Effect of beam oscillating pattern on weld characterization of laser welding of AA6061-T6 aluminum alloy. Mater. Des. 108, 707–717. https://doi.org/10.1016/j.matdes.2016.07.053. Available at.

Wang, N., et al., 2004. Solidification cracking of superalloy single- and bi-crystals. Acta Mater. 52 (11), 3173–3182. https://doi.org/10.1016/j.actamat.2004.03.047. Available at.

Wang, W., et al., 2020. A new test method for evaluation of solidification cracking susceptibility of stainless steel during laser welding. Materials (Basel) 13 (14), 3178. https://doi.org/10.3390/ma13143178. Available at.

Wei, H.L., Elmer, J.W., Debroy, T., 2016. Origin of grain orientation during solidification of an aluminum alloy. Acta Mater. 115, 123–131. https://doi.org/10.1016/j.actamat.2016.05.057. Available at.

Weigl, M., Albert, F., Schmidt, M., 2011. Enhancing the ductility of laser-welded copper-aluminum connections by using adapted filler materials. Phys. Procedia 335–341. https://doi.org/10.1016/j.phpro.2011.03.141. Available at.

Woizeschke, P., et al., 2017. Laser deep penetration welding of an aluminum alloy with simultaneously applied vibrations. Lasers Manuf. Mater. Process. 4 (1), 1–12. https://doi.org/10.1007/s40516-016-0032-9. Available at.

Xu, C., et al., 2016. Evolution of microstructure, mechanical properties and corrosion resistance of ultrasonic assisted welded-brazed Mg/Ti joint. J. Mater. Sci. Technol. 32 (12), 1253–1259. https://doi.org/10.1016/j.jmst.2016.08.029. Available at.

Xue, X., Wu, X., Liao, J., 2021. Hot-cracking susceptibility and shear fracture behavior of dissimilar Ti6Al4V/AA6060 alloys in pulsed Nd:YAG laser welding. Chin. J. Aeronaut. 34 (4), 375–386. https://doi.org/10.1016/j.cja.2020.12.015. Available at.

Yan, S., et al., 2022. Experimental study on the grain evolution induced by thermal characteristics during oscillation laser welding of IN718. Mater. Lett. 323. https://doi.org/10.1016/j.matlet.2022.132581. Available at.

Yao, Z., et al., 2022. Equiaxed microstructure formation by ultrasonic assisted laser metal deposition. Manuf. Lett. 31, 56–59. https://doi.org/10.1016/j.mfglet.2021.07.002. Available at.

Yu, X.Y., et al., 2016. Fiber laser welding of WC-Co to carbon steel using Fe-Ni Invar as interlayer. Int. J. Refract. Met. Hard Mater 56, 76–86. https://doi.org/10.1016/j.ijrmhm.2015.12.006. Available at.

Zhang, P., et al., 2021. A review on the effect of laser pulse shaping on the microstructure and hot cracking behavior in the welding of alloys. Optics and Laser Technology. Elsevier Ltd. https://doi.org/10.1016/j.optlastec.2021.107094. Available at.

Zhang, Y., et al., 2015. Reduced hot cracking susceptibility by controlling the fusion ratio in laser welding of dissimilar Al alloys joints. J. Mater. Res. 30 (7), 993–1001. https://doi.org/10.1557/jmr.2015.64. Available at.

Zhang, Y., et al., 2016. Investigation on the effects of parameters on hot cracking and tensile shear strength of overlap joint in laser welding dissimilar Al alloys. Int. J. Adv. Manuf. Technol. 86 (9–12), 2895–2904. https://doi.org/10.1007/s00170-016-8383-0. Available at.

Zhao, X.J., et al., 2011. η phase formation mechanism at cemented carbide YG30/steel 1045 joints during tungsten-inert-gas arc welding. Materials Science Forum. Trans Tech Publications Ltd, pp. 901–904. https://doi.org/10.4028/www.scientific.net/MSF.675-677.901. Available at.

Zhou, S., et al., 2021. Follow-up ultrasonic vibration assisted laser welding dissimilar metals for nuclear reactor pump can end sealing. Nucl. Mater. Energy 27. https://doi.org/10.1016/j.nme.2021.100975. Available at.

Zuo, D., et al., 2014. Intermediate layer characterization and fracture behavior of laser-welded copper/aluminum metal joints. Mater. Des. 58, 357–362. https://doi.org/10.1016/j.matdes.2014.02.004. Available at.